Published in final edited form as:
Anal Chem. 2005 May 15; 77(10): 3173–3182.

Reagent Anions for Charge Inversion of Polypeptide/Protein Cations in the Gas Phase

Min He, **Joshua F. Emory**, and **Scott A. McLuckey***
Department of Chemistry, Purdue University, West Lafayette, Indiana 47907-1393

Abstract

Various reagent anions capable of converting polypeptide cations to anions via ion/ion reactions have been investigated. The major charge inversion reaction channels include multiple proton transfer and adduct formation. Dianions composed of sulfonate groups as the negative charge carriers show essentially exclusive adduct formation in converting protonated peptides and proteins to anions. Dianions composed of carboxylate groups, on the other hand, show far more charge inversion via multiple proton transfer, with the degree of adduct formation dependent upon both the size of the polypeptide and the spacings between carboxylate groups in the dianion. More highly charged carboxylate-containing anions, such as those derived from carboxylate-terminated polyamidoamine half-generation dendrimers show charge inversion to give anion charges as high in magnitude as −4, with the degree of adduct formation being inversely related to dendrimer generation. All observations can be interpreted on the basis of charge inversion taking place via a long-lived chemical complex. The lifetime of this complex is related to the strengths and numbers of the interactions of the reactants in the complex. Calculations with model systems are fully consistent with sulfonate groups giving rise to more stable complexes. The kinetic stability of the complex can also be affected by the presence of electrostatic repulsion if it is multiply charged. In general, this situation destabilizes the complex and reduces the likelihood for observation of adducts. The findings highlight the characteristics of multiply charged anions that play roles in determining the nature of charge inversion products associated with protonated peptides and proteins.

The gas-phase chemistry of ionized peptides and proteins, in conjunction with mass spectrometry, plays an important role in identifying and characterizing proteins and protein complexes. Ionization methods capable of producing ions from large poly-atomic molecules[1–3] serve an essential role in the overall process. Among the ionization methods, matrix-assisted laser desorption/ionization (MALDI)[2,3] and electrospray ionization (ESI)[1] are the principle ones in use for peptides and proteins. In the positive ionization mode, MALDI yields mainly singly protonated molecules over a wide range of polypeptide size. However, singly charged macro-ions, particularly large polypeptide and protein ions, often provide limited structural information via gas-phase fragmentation induced by commonly available ion activation methods. On the other hand, ESI typically shows a much higher propensity for the formation of multiply charged ions. In fact, a distribution of charge states is commonly formed by ESI from molecules capable of accommodating multiple charges. This can be desirable for protein identification/characterization because studies have demonstrated that the structural information available from gas-phase fragmentation can be highly sensitive to parent ion charge state.[4–8] Furthermore, it has also been observed that fragmentation of ions of opposite polarity can provide complementary structural information.[9] However, the interrogation of the same protein/polypeptide in both ion polarity modes is rarely done. In those cases in which complementary information can be obtained via analysis in both polarity modes, doing so is complicated by the requirement for separate optimization of ionization and analysis conditions.

* To whom correspondence should be addressed. Phone: (765) 494-5270. Fax: (765) 494–0239. E-mail:mcluckey@purdue.edu..

It is often the case that ionization yields differ significantly with ionization polarity mode. Hence, it is often not straightforward to access the structural information potentially available from ions of both polarities. It is, therefore, desirable to be able to manipulate ion charge states and polarities independent of the initial ionization conditions.

Several approaches have been developed to manipulate charge states of multiply charged macro-ions formed via ESI, including manipulations of solution conditions[10] and the use of ion chemistry to reduce ion charge in the gas phase.[11–14] Among the latter, ion/ion reactions have proven to be particularly well-suited to charge-state manipulation in the gas phase.[11–13,15–17] The highly exothermic nature of virtually all ion/ion reactions makes them efficient in reducing charge states of macro-ions to arbitrarily low values.[18] Furthermore, use of appropriate reagent ions can avoid clustering reactions, which are often observed with the use of ion/molecule reactions intended to lead to proton transfer.[18,19] Most detailed studies have been conducted within the context of a tandem mass spectrometry experiment in quadrupole ion traps. A number of analytically useful measurements involving protein ion charge-state manipulation in ion traps have been demonstrated.[5–7,20] These include, for example, the use of ion/ion reactions to simplify mass spectra of protein mixtures,[6,21,22] to simplify protein product ion spectra derived from multiply charged parent ions,[5–7,23,24] and to concentrate ions into a single charge state.[25]

The ion/ion reaction studies reported to date have mainly involved the use of singly charged reagent ions that give rise to a single proton-transfer reaction. The reduction of protein charge by more than one charge state requires sequential ion/ion reactions. Although this one-charge change per step approach is highly effective for charge-state reduction, it is not appropriate for changing the polarity of the protein ion. Some methods have been demonstrated to be capable of changing ion polarities in the gas phase. In particular, ion/neutral collisions involving electronic transitions[26,27] have been exploited for charge-changing reactions. Most of this work has been performed on beam-type mass spectrometers where kiloelectronvolt energy ion/neutral collisions occur in a field-free region prior to one or more mass analyzers. The products of these reactions are often formed in excited electronic states. As a result, extensive fragmentation of the product ions is often observed.[26,28,29] Far more work involving the formation of positive ions from negative ions has been reported via this approach than the opposite case due, at least in part, to the relatively low cross sections associated with the latter process.[30,31] Ion/ion reactions at low relative translational energies provide an alternative to ion/neutral collisions at high translational energies for charge inversion. Ion/ion reaction cross sections are orders of magnitude larger than those of the endothermic reactions associated with the high-energy beam experiments, and they lead to little or no fragmentation, under appropriate conditions. These factors lead to relatively high charge inversion efficiencies such that it is possible to conduct sequential charge inversion studies with overall efficiencies on the order of tens of percent.[32,33]

The efficiency of charge inversion to a particular product ion via ion/ion reaction is determined both by the conversion of parent ions to products and by the partitioning of charge among the products, including neutral species. This efficiency is highly dependent upon the properties of the charge inversion reagents. Furthermore, the relative extents to which charge inversion occurs via proton transfer and via adduct formation are sensitive to the identities of the charge inversion reagents. In this work, we focus on the role of the reagent ions used to invert the charge of a polypeptide ion from positive to negative. In particular, we emphasize the tendency for charge inversion via proton transfer versus via adduct formation.

EXPERIMENTAL SECTION

Bovine ubiquitin and bradykinin were purchased from Sigma (St. Louis, MO), and their aqueous solutions (0.1 mg/mL) with 1% acetic acid were prepared and subjected to positive ion electrospray. Carboxylate-terminated polyamidoamine dendrimer (PAMAM) generations 0.5, 1.5, 2.5, and 3.5 were purchased from Aldrich (Milwaukee, WI) and dissolved in 2% aqueous ammonium hydroxide solution to a concentration of about 1–2 wt %. 1,3-Benzenedisulfonic acid was purchased from Aldrich and prepared in aqueous solution (1.0 mg/mL). Other reagents, including 1,4-phenylenedipropionic acid (PDPA), 2,6-naphthalenedisulfonic acid (2,6-NDSA), 2,6-naphthalenedicarboxylic acid (2,6-NDCA), and 1,4-naphthalenedicarboxylic acid (1,4-NDCA) were subjected to negative nanospray from 2% ammonium hydroxide at variable concentrations. PDPA, 2,6-NDSA, 2,6-NDCA, and 1,4-NDCA were obtained from Aldrich. Perfluro-1,3-dimethylcyclohexane (PDCH) was purchased from Aldrich (St. Louis, MO), and headspace vapors were subjected to atmospheric sampling glow discharge ionization.

All experiments were performed with modified Finnigan-ITMS quadrupole ion trap mass spectrometers coupled with homemade electrospray sources, allowing for the sequential injection and subsequent reaction of oppositely charged ions generated via electrospray ionization. One of the instruments was also modified for the injection of anions through a hole in the ring electrode. Detailed descriptions of the instruments have been provided previously.[34,35] All experiments were controlled by ICMS software.[36] Positive ions were accumulated in the ion trap followed by multiple resonance ejection steps[37] to isolate a specific charge state, when necessary. Subsequently, negative ions that served as charge inversion reagents, produced from another electrospray source, were directed into the ion trap. A mutual storage period for the ions of opposite polarities allowed for the ion/ion reactions to take place. Mass analysis was effected via resonance ejection.[38] In some cases, singly charged anions generated from PDCH were used to manipulate the charge states of protein ions prior to charge inversion reactions.

High-level density functional theory and ab initio computations were carried out to obtain the structures and energies of ions and neutral species relevant to this study using Gaussian 98[39] or Gaussian 03.[40] Geometry optimizations, including vibrational analysis were performed at the B3LYP/6-31G+(d) level.[41] All stationary points were found to be true minimums. To determine the energies of the various species, single-point energy calculations were performed at the MP2(full)/6-311+G(2d,2p) level using the B3LYP/6-31G+(d) optimized geometries. Thermal energy corrections were scaled by a factor of 0.9804.[41] The values reported herein have been subjected to zero-point energy correction.

RESULTS

Reagent anions for the charge inversion of protonated polypeptides must carry at least two charges and should be readily formed with relatively high abundances to minimize reaction times. We have examined compounds with a variety of functionalities that facilitate negative ion formation in electrospray ionization. All of the general phenomenology noted for charge inversion can be summarized with compounds composed of either multiple sulfonate or carboxylate functionalities. The results described herein, therefore, are restricted to cases using carboxylic and sulfonic acids as reagents.

Charge Inversion of Peptide Ions via Dicarboxylic versus Disulfonic Acids

Doubly deprotonated ions are readily formed by negative electrospray ionization of 2,6-NDSA and 2,6-NDCA. These anions have been subjected to reactions with both singly charged peptides and multiply charged proteins. The results for the reaction of singly protonated

bradykinin (RPPGFSPFR) with the dianions of these acids are cases in point. In both cases, when the $[M + H]^+$ ions were reacted with $[2,6\text{-NDSA-2H}]^{2-}$ and $[2,6\text{-NDCA-2H}]^{2-}$, respectively, peptide ion charge inversion took place but the products were distinct. Charge inversion with 2,6-NDSA dianions occurred exclusively via complex formation, whereas charge inversion with 2,6-NDCA dianions occurred exclusively by proton transfer to form deprotonated bradykinin. Hence, it is apparent that 2,6-NDCA is the more appropriate choice for charge inversion via proton transfer and that 2,6-NDSA is the more appropriate choice for charge inversion via anion attachment. (Note that the same behavior was noted for other positional isomers of these reagents.)

Charge Manipulation of Protein Ions with Dianions of Disulfonic Acids

Figure 1 summarizes data collected for the reaction of the $[U + 7H]^{7+}$ ion derived from bovine ubiquitin, U, with dianions derived from 1,3-benzenesulfonic acid (BDSA). The positive ion spectrum from *m*/*z* 2000 to *m*/*z* 10000 derived after a reaction period of 500 ms is shown in Figure 1a. The three major products are $[U + 2BDSA + 3H]^{3+}$, $[U + 2BDSA + 2H]^{2+}$, and $[U + 3BDSA + H]^+$. The $[U + 2BDSA + 3H]^{3+}$ and $[U + 3BDSA + H]^+$ ions are formed from sequential attachment of two or three dianions of BDSA, respectively, to the $[U + 7H]^{7+}$ ion. It is noteworthy that these ions are the only abundant products at these charge states, indicating that BDSA attachment is, by far, the dominant reaction process. A single proton-transfer step must take place for the formation of the $[U + 2BDSA + 2H]^{2+}$ ion. At short reaction times, a significant abundance of the $[U + 6H]^{6+}$ ion was noted (data not shown) due to a proton tunneling mechanism for charge transfer, as discussed further below. The attachment of two BDSA dianions after the proton tunneling step is likely to give rise to most of the $[U + 2BDSA + 2H]^{2+}$ product.

Very similar behavior was noted for dianions derived from NDSA (data not shown). By increasing the mutual storage time between the two reaction partners, the ion/ion reaction went further and the negative complex, $[U + 4BDSA - H]^-$, was observed, as shown in Figure 1b. Essentially no charge inversion via two-proton transfer is noted. A second charge inversion step was performed with this system whereby the negative ions in Figure 1b were isolated and subjected to ion/ion reaction with $[U + 7H]^{7+}$ ions, which were reintroduced into the ion trap. The reaction gave rise to the essentially exclusive formation of a six-body complex, $[2U + 4BDSA + 6H]^{6+}$, depicted in Figure 1c. This product, therefore, was formed from five consecutive ion/ion reactions involving anion/cation attachment.

Figure 2 summarizes experiments that shed light on some of the major sequential reaction pathways associated with reactions of $[U + 7H]^{7+}$ cations with dianions. Figure 2a shows the positive ion product ion spectrum obtained after the reaction of $[U + 7H]^{7+}$ cations with dianions derived from 2,6-NDSA over a relatively short reaction time. Over the displayed *m*/*z* range, product ions ranging in charge from +6 to +3 are evident. In the case of the +6 products, the $[U + 6H]^{6+}$ ion dominates with a much lesser abundance of the $[U + NDSA + 6H]^{6+}$ ion. A relatively high amplitude dipolar sine-wave voltage that corresponded roughly to the frequencies of the +6 ions was applied during the ion/ion reaction period so that both of the +6 products would be prevented from engaging in subsequent reactions by ejecting them from the ion trap. As shown in Figure 2b, the formation of the +5 product ions was relatively little perturbed while both the +6 and 4+ products were largely eliminated. (Note that the amplitude needed to eject almost all of the +6 ions also led to the ejection of some of the +5 ions via off-resonance power absorption.) The decrease in +4 ion signals indicates that the +4 ions are largely formed from sequential reactions involving the +6 ions. The +4 signal that does appear may result largely from signal proton transfer from the +5 ions. As expected, relatively little of the +5 product ion population is formed from sequential reactions from the +6 ions. Rather, they are largely formed via a one-step reaction between the $[U + 7H]^{7+}$ cations and NDSA

dianions. Figure 2c shows the experiment in which a dipolar sine wave in resonance with the $[U + NDSA + 5H]^{5+}$ ion was applied to inhibit its subsequent reactions. In this case, since there is only one major +5 ion, a lower amplitude signal could be used to inhibit the sequential reactions of +5 ions. This approach, referred to as ion parking,[25] allows for the inhibition of the ion/ion reactions of the ion undergoing excitation without ejecting it from the ion trap. In this case, the major effect is the decreased formation of the $[U + 2NDSA + 3H]^{3+}$ product. Experiments such as these were used to demonstrate that the odd charge-state products formed from $[U + 7H]^{7+}$ cations and all of the dianions investigated in this study were largely formed via the sequence of $+7 \rightarrow +5 \rightarrow +3 \rightarrow +1 \rightarrow -1$. Even electron products mostly arose from the sequence $+7 \rightarrow +6 \rightarrow +4 \rightarrow +2$, where the first step involves a single proton transfer from $[U + 7H]^{7+}$ to the dianion, presumably via the tunneling mechanism, without adduct formation.

Charge Manipulation of Protein Ions with Dianions of Dicarboxylic Acids

Figure 3 summarizes ion/ion reaction behavior noted for the reaction of $[U + 7H]^{7+}$ ions with dianions derived from the negative ion electrospray of 1,4-phenylenedipropionic acid (PDPA). Figure 3a shows the positive ion spectrum over the *m*/*z* range of 1200–2400 after a relatively short reaction time. Figure 3b shows positive ion products over the *m*/*z* range of 2500–8500 after a somewhat longer reaction time. It is clear that both proton transfer and attachment of PDPA anions take place to form protonated ubiquitin ions, $[U + nH]^{n+}$ (n = 1–6), and anion attachment to generate complexes, $[U + aX + mH]^{m+}$ (a = 1–3; m = 1–6), where X represents the neutral PDPA molecule. The appearance of an abundant $[U + 6H]^{6+}$ ion confirms that single proton transfer takes place, as was observed with the other dianions. This process also forms singly deprotonated PDPA anions, which can, in turn, engage in subsequent ion/ion reactions. For example, the attachment of $[PDPA - H]^-$ anions to the $[U + 7H]^{7+}$ ions likely accounts for the small signal corresponding to the $[U + X + 6H]^{6+}$ ion. The +5 products arise predominantly from single-step reactions, as indicated by experiments of the kind described in conjunction with Figure 2. In this case, the transfer of two protons to the PDPA dianion, presumably via a chemical complex, gives rise to the $[U + 5H]^{5+}$ product whereas the adduct represents a stabilized form of the chemical complex that likely represents an intermediate in the formation of $[U + 5H]^{5+}$. (Collisional activation of the $[U + mX + nH]^{n+}$ complexes lose one or more molecules of X.) Although complexes tend to dominate the total product ion population as charge state decreases, the abundance of the complex, $[U + X + nH]^{n+}$ (n = 1–6), exceeds that of $[U + nH]^{n+}$ (n = 1–6) in the odd-charge states while for the even-charge states, the relative abundances of the $[U + nH]^{n+}$ ions are greatest. This reflects the predominant reaction pathways discussed above for the even- and odd-charge products. That is, the even-charge products involve at least one single proton-transfer step, thereby increasing the relative abundance of the $[U + nH]^{n+}$ product.

With a longer ion/ion reaction period, charge inversion products were observed in the negative ion detection mode, as shown in Figure 3c. The relative abundances of the −1 products mirror those of the +1 products in Figure 3b, but they all contain one more molecule of PDPA than the corresponding +1 ion. That is, the relative abundance of the $[U + H]^+$ cations (see Figure 3b) corresponds with the relative abundance of the $[U + X - H]^-$ ion, the relative abundance of the $[U + X + H]^+$ ion corresponds with that of $[U + 2X - H]^-$ ion, and so forth. This indicates that, in the charge inversion step, attachment of PDPA dianions predominates over the transfer of two protons. This stands in contrast to the behavior of carboxylate dianions with singly protonated bradykinin, where the $[M + H]^+$ was converted to $[M - H]^-$ anions with no adduct ion formation. Exclusive proton transfer was also observed for PDPA dianions in reaction with protonated bradykinin (data not shown). The similar behaviors of the PDPA and NDCA dianions with protonated bradykinin indicate that the different charge inversion behavior of PDPA dianions with protonated ubiquitin is largely due to differences between the peptide and protein. As discussed further below, differences in reactivity are likely to be due to the

availabilities and strengths of relatively strong noncovalent interactions in the charge inversion products.

While it is clear from the behavior of PDPA dianions in reactions with ubiquitin and bradykinin cations that the nature of the polypeptide cation influences the extent to which adduct formation is observed in reactions with carboxylate dianions, the nature of the dianion also apparently plays a role. This is illustrated in Figure 4, which summarizes data for the reaction of $[U + 7H]^{7+}$ cations with dianions derived from 2,6-NDCA. Figure 4a shows the positive ion spectrum over the *m*/*z* range of 1000–3000 after a relatively short ion/ion reaction period, and Figure 4b shows the positive ion spectrum over the *m*/*z* range of 2000–10 000 acquired after a longer ion/ion reaction period. Clearly, much less adduct formation is noted for NDCA than for PDPA (compare Figure 4a and b with Figure 3a and b). The closer proximity of the negative charges in NDCA likely plays a role here either via a greater degree of electrostatic repulsion or the limited ability to engage in two simultaneous interactions with the polypeptide, or a combination of these factors. With longer reaction time, the charge inversion products were observed, shown in Figure 4c. Both deprotonated and complexed ubiquitin product ions are observed, with the anion attachment dominating the charge inversion process. The observation that charge inversion mainly proceeded via anion attachment, regardless of the fact that much less anion attachment has been observed when reducing the charge states of ubiquitin ions in the same polarity, can be accounted for by considering the different interaction sites and strengths, as explained below.

Charge Manipulation of Protein Cations with Multiply Charged PAMAM Dendrimer Anions

Carboxylate dianions consistently show lower degrees of adduct formation than sulfonate dianions. However, in either case, only singly charged product anions can be formed via charge inversion of polypeptide cations. Furthermore, due to the limited *m*/*z* range over which ions of opposite polarity can be stored in an electrodynamic ion trap, it is desirable to identify relatively high mass anionic reagents for the charge inversion of high-mass singly charged polypeptides. We therefore examined polymeric species with multiple carboxylate groups to investigate both the degree of adduct formation and the extent to which multiple charging takes place upon charge inversion. Specifically, we have examined carboxylate-terminated dendrimers, i.e., regularly branched polymers with a dendritic, treelike structure.[42,43] Here, we chose PAMAM dendrimers for study. These molecules can be synthesized in large quantities and have been studied extensively by several research groups.[44,45] Half-generation PAMAM dendrimers can be terminated in carboxylate groups, and as a result, it is possible to generate multiply charged negative ions from them via electrospray.[46] Furthermore, the number of acidic groups on the surface of the dendrimer doubles with each generation. Therefore, anions over a relatively wide range of charge states can be formed by use of different PAMAM dendrimer generations.

In preliminary reports, PAMAM dendrimer generation 0.5 anion summarizes charge inversion experiments involving $[U + H]^+$ ions and anions derived from a series of PAMAM dendrimer generations ranging from 0.5 to 3.5. The $[U + H]^+$ ions were formed via a series of single proton-transfer reactions from multiply charged ubiquitin cations to singly charged anions derived from glow discharge ionization of perfluoro-1,3-dimethylcyclohexane. In each case, all anions derived from the PAMAM dendrimer samples were allowed to react with the protein cations. Data collected for low-generation PAMAM dendrimer samples showed a complex mixture of species including a distribution of charge states with mixtures of sodium and proton counterions, as well as ions arising from synthesis failure products.[46] The spectra of the higher generation PAMAM dendrimers were so complex that only broad ill-resolved signals were recorded. With the present instrumentation, it is difficult to isolate independently both cationic and anionic reactants. Nevertheless, it is possible to make useful observations regarding the

overall reactivities of the dendrimer anions by allowing the entire population to react. For every PAMAM generation, ubiquitin anions with charges up to −4 are clearly observed (see Figure 5). Higher charge states may also have been formed with anions from the highest generation dendrimers. However, they were precluded from observation by the residual dendrimer anions in the spectrum. Adduct formation dominates the charge inversion products formed from the PAMAM generation 0.5 anion (Figure 5a). In contrast, little or no adduct ion formation is noted as arising from reactions with the generation 1.5, 2.5, and 3.5 anions.

DISCUSSION

The data presented herein demonstrate that a key characteristic of a reagent used to invert the charge of a polypeptide cation is the extent to which it leads to attachment versus multiple proton transfer. Sulfonate-containing anions show a much higher tendency for attachment than carboxylate-containing anions, for example. It was also noted that 1,4-phenylenedipropionate dianions showed a greater tendency for attachment to ubiquitin cations than did 2,6-naphthalenedicarboxylate anions. Furthermore, PAMAM generation 0.5 anion showed a much higher tendency for attachment to singly protonated ubiquitin ions than did anions derived from the higher generations. Each of these observations is discussed below. However, to provide context within which these results can be considered, we present a discussion of the factors that, in general, underlie ion/ion charge inversion reactions.

The magnitudes and charge-state dependencies of ion/ion reaction rates in the quadrupole ion trap under near-thermal energy conditions are consistent with the formation of an orbiting pair bound by the electric field of the oppositely charged reactants as the rate-determining step.[30] Recent studies involving multiply charged cations reacting with multiply charged anions revealed that, once the orbiting pair has been formed, two distinct mechanisms for charge transfer between reactants can be operative.[47] One involves the formation and subsequent dissociation of a long-lived complex in which the reactants come into intimate contact and the other involves charge transfer, typically in the form of proton transfer, without the formation of a long-lived “chemical” complex. The former mechanism is analogous to ion/molecule proton-transfer reactions at thermal energies in that a long-lived intermediate is formed.[48] The latter mechanism arises from the relatively high electric fields associated with oppositely charged ions as they approach one another that allows for a proton to transfer over distances sufficiently long to avoid formation of a complex. This mechanism is referred to herein as “proton hopping”. The kinetic scheme associated with the simplest case for charge transfer of a cation of a species of interest, M, is shown

in Scheme 1 for the reaction of a singly protonated ion with a doubly deprotonated reagent species:

$$(M + H)^{+} + (R - 2H)^{2-} \rightarrow \text{products} \quad (1)$$

The scheme shows a rate constant for the formation of the ion/ion pair, k_{pair}. The orbits within the population of ion/ion pairs range from circular to highly elliptical, and the nature of the orbit is believed to play a role in the relative likelihood for proton tunneling versus formation of a chemical complex. The rate constant for proton tunneling or “hopping” that, in this case, leads to the neutralization of $(M+H)^{+}$, is represented by k_{hop}.

The rate constant for formation of a long-lived chemical intermediate is represented by k_c. Three main possibilities exist for the fate of the excited chemical intermediate: (1) relaxation to yield a stable complex, (2) single proton transfer to lead to a neutralization of the cation, thereby giving rise to the same set of products yielded by the proton hopping mechanisms, and

(3) double proton transfer to lead to neutralization of the reagent anion and charge inversion of the cation.

The kinetic scheme for the general case of charge inversion of cations to anions, represented by the reaction

$$(\mathrm{M} + m\mathrm{H})^{m+} + (\mathrm{R} - n\mathrm{H})^{n-} \rightarrow \text{products} \quad (2)$$

where $|n| > |m|$, is shown in Scheme 2. This scheme is analogous to that of the simplest case, but many additional channels are available for the partitioning of charge for both charge-transfer mechanisms. In the case of the proton tunneling mechanism, there are m possible channels for proton transfer under the influence of the field of oppositely charged ions. In the case of dissociation of the excited long-lived intermediate, there are $n - m + 1$ possible channels, excluding those associated with the separation of oppositely charged fragments.

The latter reactions require much more energy than those channels that give rise to either two products of negative polarity or a negatively charged product and a neutral product and can be excluded from consideration. There are two possible channels that give rise to a negative ion and a neutral species, and these correspond to the neutralization of either M or R. The neutralization of R represents the greatest number of proton transfers from M and gives rise to the maximum negative charge state of M. There are $n - m - 1$ possible channels that give rise to two negatively charged products. Each of these channels results in an inversion of the polarity of M.

Neither Scheme 1 nor Scheme 2 shows charge inversion to occur via a hopping mechanism. This mechanism is unlikely to contribute significantly to charge inversion because the high electric field associated with the approach of oppositely charged ions is absent when M is neutralized. At this point, the interaction potential becomes that of an ion/molecule reaction, for which proton transfer is normally pictured as proceeding via a long-lived complex.[48] The significance of the proton tunneling mechanism for charge inversion lies in its role in determining the overall charge inversion efficiency. Proton tunneling can divert reactant ions from formation of a long-lived complex from which proton-transfer reactions can lead to charge inversion.

Total charge inversion efficiency can be defined as the fraction of cations derived from M that are converted to anions related to M. Charge inversion efficiency for a given channel can be defined as the fraction of reactant cations derived from M that are converted to a specific negative ion related to M. This product may be a singly or multiply deprotonated form of M or it may be a negatively charged complex that contains M. From the standpoint of charge inversion efficiency, it is desirable to minimize proton tunneling, because this process does not lead directly to charge inversion. In some cases, it is difficult to distinguish products due to proton tunneling from those due to dissociation of an excited long-lived complex, as is the case of for the neutralization of a singly charged cation (see Schemes 1 and 2). However, partial neutralization reactions are expected to arise from proton tunneling and they can sometimes be clearly identified, if present, in reactions of multiply charged ions of opposite polarity (see Figures 1–4). The factors underlying the relative propensities for complex formation versus proton tunneling are the subject of ongoing study. However, it is already apparent that the degree to which proton tunneling competes with formation of a chemical complex depends on the charges and physical sizes of the reactant ions. In these studies, proton tunneling was clearly identified as a significant process only for the $[\mathrm{U} + 7\mathrm{H}]^{7+}$ ion in reaction with dianions. It therefore likely contributed little to the charge inversion reactions involving singly protonated polypeptides and the dianions. No firm conclusions can be drawn regarding proton tunneling in the case of protonated ubiquitin and the multiply charge PAMAM anions. However,

relatively large physical cross sections of the reactants are expected to minimize the likelihood for extensive proton tunneling.

Charge inversion efficiency is also affected by competitive processes that take place via the long-lived complex. For example, it is desirable to minimize neutralization of M in the breakup of the excited complex (see Schemes 1 and 2). Furthermore, if the objective is to form deprotonated M ions, it is also desirable to minimize formation of a stable complex composed of M and R. The partitioning of products formed via the excited complex route can be discussed with reference to a Brauman-type diagram[49,50] that plots the energy as the reactants form a complex and proceed on to proton-transfer products. For example, Brauman-type diagrams that apply to the formation of an excited chemically bound complex from the ion/ion pair relevant to Scheme 1 are shown in Figure 6 for the reactions of protonated glycine with dianions derived from 2,6-NDSA^{2-}, 2,6-NDCA^{2-}, and 1,4-NDCA^{2-}.

Using ab initio methods, we have determined relevant thermodynamic values for the ion/ion reactions of 2,6-NDSA^{2-}, 2,6-NDCA^{2-}, and 1,4-NDCA^{2-} with protonated glycine serving as a model peptide cation. The structures of various dianions, protonated glycine, possible complex intermediates, as well as the neutralized anions, and singly deprotonated glycine were optimized to be the minimum energy structures. The entrance channel follows an attractive potential for ions of opposite polarity. The exit channels for charge inversion follow the potential of an ion/molecule reaction. (The potentials for the entrance and exit channels have different reactant distance dependences, i.e., r^{-1} for the entrance channel and r^{-4} for the exit channel (without permanent dipole).) Dashed lines in the exit channel are intended to allow for the possibility of barriers in the exit channels. While kinetic barriers may well be present with some combinations of M and R ions, which could lead to an increase in the kinetic stability of a complex, in the absence of a priori information about the presence of such barriers, the first approximation is to assume that they are either absent or are very similar for the two channels. Therefore, the values presented here for the difference in energy between the complex and the products represent minimum values. However, since we are most interested in comparing well depths associated with sulfonate versus carboxylate functionalities, any barriers to dissociation are expected to be similar. The well depth of the excited complex, with respect to dissociation to products, is defined by the channel that leads to the most thermodynamically stable products (again, assuming low or equal kinetic barriers in the exit channels). The well depth of the excited complex is particularly important in determining the extent to which stable complexes are observed. As the well depth increases, the lifetime of the excited complex is expected to increase such that cooling by collisions with background gases and IR emission can compete with dissociation of the complex.[51] Hence, chemical functionalities in both the cations and anions can play important roles in establishing well depths, which, in turn, play major roles in determining if charge inversion products are observed as deprotonated species or as components of stable complexes. Other important factors in determining the lifetime of the excited complex include the initial energy content of the complex and the number of degrees of freedom.

As demonstrated in Figure 6, potential surfaces “a” and “b” represent the reactions between glycine cation and 2,6-NDCA and 1,4-NDCA dianions, respectively, while potential surface “c” is associated with energies for the glycine cation/2,6-NDSA dianion case. The energies associated with the carboxylate dianions are similar to one another but they differ significantly from those of the sulfonate anion. For example, the energy difference between the reactants and the complex is calculated to be about −364 kcal/mol in the NDSA case and roughly −395 and 30 kcal/mol for each of the NDCA cases. More importantly, with respect to the issue of adduct formation, the well depth for the dissociation of the complex for the NDSA case is ~51 kcal/mol while the well-depths are roughly 30 and 25 kcal/mol, respectively, for the 2,6-NDCA and 1,4- NDCA ions. The calculations are therefore qualitatively consistent with observation

in that the complexes with carboxylate anions are less kinetically stable and, as a result, tend to show greater degrees of proton transfer relative to adduct formation.

It was noted that, for PDPA and NDCA anions, adduct formation and proton transfer competed while the ubiquitin ions were positive in polarity but that adduct formation dominated for the charge inversion step. The charge inversion step is more likely to give rise to adduct formation due to the availability of a new and stronger noncovalent interaction. That is, positive ions are presumably composed of one or more protonated basic residues. If present, any deprotonated sites are likely to be stabilized by a salt bridge.[52–54] Therefore, in the reaction of dianions with cations with two or more positive charges, acid–base interactions are likely to dominate in the adducts.[55] That is, interactions of the form R–COOH---H_2N–R′, are likely to be involved. In the case of the charge inversion step leading to a net charge of −1, a proton-bound dimer interaction becomes possible, i.e., R–COO^----H^+--$^-$OOC–R′. The proton-bound dimer interaction was found to be roughly 7–17 kcal/mol more stable than the corresponding acid–base interaction. The values listed in Figure 6 are therefore based on a proton-bound complex structure. However, it is noteworthy that the strengths of the acid–base interactions follow the same qualitative order for the sulfonic and carboxylic acids. Therefore, adduct formation within the ubiquitin positive ion polarity sequence +7 → +5 → +3 → +1 is expected to be greater for NDSA than for NDCA, as observed. The greater tendency for adduct formation between ubiquitin cations and PDPA dianions than was noted for NDCA anions most likely arises from the spacing and additional flexibility of the carboxylate groups. The acidic functionalities are the same and the sizes of the molecules are not dramatically different. However, the greater spacing between carboxylate groups in the PDPA dianion may facilitate the interactions of both functionalities simultaneously with the protein, thereby increasing the well depth of the complex.

The energy diagram associated with the ion/ion reaction intermediate for the case of $[U + H]^+$ reacting with PAMAM dendrimer ions of charge greater than |−2| is more complex than that of Figure 6. While some doubly charged PAMAM anions may have contributed to the results of Figure 5, most of the anions were of higher absolute charge. In general, $(M + mH)^{m+}$ ions reacting with $(R - nH)^{n-}$ ions, where $|n| > |m|$, is significantly more complex than that of the simplest case described above whenever $|n|$ exceeds $|m|$ by two or more. In these cases, proton-transfer channels in addition to those leading to neutralization of M and R become available. Furthermore, the energy surfaces of the additional reactions follow those of the dissociation of a multiply charged ion into two products of like charge. Such reactions inherently have kinetic barriers, sometimes referred to as Coulomb barriers, associated with the separation of like charges.[56,57] However, electrostatic repulsion tends to favor these channels, at least on thermodynamic grounds. A hypothetical energy diagram for the simplest case for the condition where $|n|$ exceeds $|m|$ by two or more applies to the reaction of $(M + H)^+$ with $(R - 3H)^{3-}$, and is shown in Figure 7.

This diagram shows an exit channel with charge separation, which distinguishes this type of reaction from those in which $|n|$ exceeds $|m|$ by one (see Figure 6). The diagram shows the charge separation barrier to be lower than those that follow an ion/molecule reaction surface. In general, charge separation reactions from multiply charged ions tend to be favored over dissociation reactions involving neutral loss, particularly for highly charged species. The simplest interpretation for the data of Figure 5 is that, as the PAMAM generation increases, the charges of the dendrimer anions increase, which was clear from the negative ESI of the dendrimers (data not shown), such that charge separation channels increasingly dominate as dendrimer generation increases. Electrostatic repulsion associated with these channels is likely to decrease dissociation barriers relative to those of either of the channels that lead to neutralization of either the protein or the dendrimer. The likelihood for adduct formation is therefore expected to decrease with increasing anion charge, as is observed experimentally (see

Figure 5). This tendency suggests that highly charged anions should be used for the charge inversion of singly charged cations. However, it is also expected that the likelihood for proton tunneling increases with anion charge, which may impose a compromise condition. In the case of the charge inversion of protonated ubiquitin with PAMAM dendrimers, no evidence that such a condition was reached with anions derived from PAMAM dendrimer generation 3.5 was apparent.

CONCLUSIONS

Protonated peptides and proteins can be converted to negative ions via the transfer of multiple protons to multiply charged anions or via attachment of an anion to form a complex. The chemical functionalities associated with the anion charge sites play a major role in determining if charge inversion takes place via complex formation or via multiple proton transfer. Anions with sulfonate groups show a high propensity for adduct formation whereas anions with carboxylate groups are more likely to show charge inversion via multiple proton transfer. These findings are consistent with the strengths of the interactions within the long-lived intermediates that lead to proton transfer. At least for some carboxylate anions, both proton transfer and adduct formation are observed. Adduct formation, in these cases, appears to be most likely when the structure of the anion is such that simultaneous interactions of the carboxylate groups with the polypeptide are favored and when the complex is not electrostatically destabilized. The formation of multiply deprotonated polypeptides from protonated peptides can be accomplished in a single ion/ion collision using multiply charged anions derived from carboxylate terminated PAMAM dendrimers. Ubiquitin anions with negative charge as high as −4 were formed with anions derived from each dendrimer generation investigated. Adduct formation was minimized by use of the larger dendrimers, which tend to yield highly charged reagent anions. These findings provide informational insights into the characteristics of anions that determine the nature of the products formed in an ion/ion charge inversion experiment involving peptides and proteins.

Acknowledgements

The authors acknowledge key contributions in the design and fabrication of the instrumentation used in this work by Mr. Chris Doerge of the Amy Instrumentation Facility, Dr. J. Mitchell Wells, and Dr. Ethan R. Badman. This research was sponsored by the National Institutes of Health under Grant GM 45327 and the U.S. Department of Energy under Award DE-FG02-00ER15105.

References

1. Fenn JB, Mann M, Meng CK, Wong SF, Whitehouse CM. Science 1989;246:64–71. [PubMed: 2675315]
2. Hillenkamp F, Karas M, Beavis RC, Chait BT. Anal Chem 1991;63:1193A–1202A. [PubMed: 1897719]
3. Karas M, Hillenkamp F. Anal Chem 1988;60:2299–2301. [PubMed: 3239801]
4. Dongre AR, Jones JL, Somogyi A, Wysocki VH. J Am Chem Soc 1996;118:8365–8374.
5. Reid GE, Wu J, Chrisman PA, Wells JM, McLuckey SA. Anal Chem 2001;73:3274–3281. [PubMed: 11476225]
6. Reid GE, Shang H, Hogan JM, Lee GU, McLuckey SA. J Am Chem Soc 2002;124:7353–7362. [PubMed: 12071744]
7. He M, Reid GE, Shang H, Lee GU, McLuckey SA. Anal Chem 2002;74:4653–4661. [PubMed: 12349967]
8. Hogan JM, McLuckey SA. J Mass Spectrom 2003;38:245–256. [PubMed: 12644985]
9. Bowie JH, Brinkworth CS, Dua S. Mass Spectrom Rev 2002;21:87–107. [PubMed: 12373746]
10. Muddiman DC, Cheng X, Udseth HR, Smith RD. J Am Soc Mass Spectrom 1996;7:697–706.
11. McLuckey SA, Van Berkel GJ, Glish GL. J Am Chem Soc 1990;112:5668–5670.

12. McLuckey SA, Glish GL, Van Berkel GJ. Anal Chem 1991;63:1971–1978. [PubMed: 1661106]
13. Loo RRO, Smith RD. J Mass Spectrom 1995;30:339–347.
14. Zubarev RA, Horn DM, Fridriksson EK, Kelleher NL, Kruger NA, Lewis MA, Carpenter BK, McLafferty FW. Anal Chem 2000;72:563–573. [PubMed: 10695143]
15. Loo RRO, Udseth HR, Smith RD. J Phys Chem 1991;95:6412–6415.
16. Scalf M, Westphall MS, Krause J, Kaufman SL, Smith LM. Science 1999;283:194–197. [PubMed: 9880246]
17. Ebeling DD, Westphall MS, Scalf M, Smith LM. Anal Chem 2000;72:5158–5161. [PubMed: 11080858]
18. Stephenson JL Jr, McLuckey SA. J Am Chem Soc 1996;118:7390–7397.
19. Stephenson JL Jr, McLuckey SA. Int J Mass Spectrom Ion Processes 1997;162:89–106.
20. Hogan JM, Pitteri SJ, McLuckey SA. Anal Chem 2003;75:6509–6516. [PubMed: 14640721]
21. Stephenson JL Jr, McLuckey SA. Anal Chem 1996;68:4026–4032. [PubMed: 8916454]
22. Stephenson JL Jr, McLuckey SA. J Am Soc Mass Spectrom 1998;9:585–596. [PubMed: 9879372]
23. Schaaff TG, Cargile BJ, Stephenson JL Jr, McLuckey SA. Anal Chem 2000;72:899–907. [PubMed: 10739190]
24. Wells JM, Stephenson JL Jr, McLuckey SA. Int J Mass Spectrom 2000;203:A1–A9.
25. McLuckey SA, Reid GE, Wells JM. Anal Chem 2002;74:336–346. [PubMed: 11811406]
26. Cooks, R. G., Ed. Collision Spectroscopy; Plenum Press: New York, 1978.
27. Danell AS, Glish GL. Int J Mass Spectrom 2001;212:219–227.
28. Bowie JH, Blumenthal T. J Am Chem Soc 1975;97:2959–2962.
29. Hayakawa S. Int J Mass Spectrom 2001;212:229–247.
30. Busch, K. L.; Glish, G. L.; McLuckey, S. A. Mass Spectrometry/Mass Spectrometry Techniques and Applications of Tandem Mass Spectrometry; VCH Publishers: New York, 1988.
31. Hayakawa, S., ASMS Conference, Nashville, TN, 2004.
32. He M, McLuckey SA. J Am Chem Soc 2003;125:7756–7757. [PubMed: 12822966]
33. He M, McLuckey SA. Anal Chem 2004;76:4189–4192. [PubMed: 15253662]
34. Wells JM, Chrisman PA, McLuckey SA. J Am Soc Mass Spectrom 2002;13:614–622. [PubMed: 12056562]
35. Badman E, Chrisman AP, McLuckey SA. Anal Chem 2002;74:6237–6243. [PubMed: 12510744]
36. ICMS software provided by N.Yates and the University of Florida.
37. McLuckey SA, Goeringer DE, Glish GL. J Am Soc Mass Spectrom 1991;2:11–21.
38. Kaiser RE, Cooks RG, Stafford GC, Syka JEP, Hemberger PH. Int J Mass Spectrom Ion Processes 1991;106:79–115.
39. Frisch, M. J.; Trucks, G. W.; Schlegel, H. B.; Scuseria, G. E.; Robb, M. A.; Cheeseman, J. R.; Zakrzewski, V. G.; Montgomery, J. A., Jr.; Stratmann, R. E.; Burant, J. C.; Dapprich, S.; Millam, J. M.; Daniels, A. D.; Kudin, K. N.; Strain, M. C.; Farkas, O.; Tomasi, J.; Barone, V.; Cossi, M.; Cammi, R.; Mennucci, B.; Pomelli, C.; Adamo, C.; Clifford, S.; Ochterski, J.; Petersson, G. A.; Ayala, P. Y.; Cui, Q.; Morokuma, K.; Malick, D. K.; Rabuck, A. D.; Raghavachari, K.; Foresman, J. B.; Cioslowski, J.; Ortiz, J. V.; Baboul, A. G.; Stefanov, B. B.; Liu, G.; Liashenko, A.; Piskorz, P.; Komaromi, I.; Gomperts, R.; Martin, R. L.; Fox, D. J.; Keith, T.; Al-Laham, M. A.; Peng, C. Y.; Nanayakkara, A.; Gonzalez, C.; Challacombe, M.; Gill, P. M. W.; Johnson, B.; Chen, W.; Wong, M. W.; Andres, J. L.; Gonzalez, C.; Head-Gordon, M.; Replogle, E. S.; Pople, J. A., Revision A.7 ed.; Gaussian, Inc.: Pittsburgh, PA, 1998.
40. Frisch, M. J.; Trucks, G. W.; Schlegel, H. B.; Scuseria, G. E.; Robb, M. A.; Cheeseman, J. R.; Montgomery, J. A., Jr.; Vreven, T.; Kudin, K. N.; Burant, J. C.; Millam, J. M.; Iyengar, S. S.; Tomasi, J.; Barone, V.; Mennucci, B.; Cossi, M.; Scalmani, G.; Rega, N.; Petersson, G. A.; Nakatsuji, H.; Hada, M.; Ehara, M.; Toyota, K.; Fukuda, R.; Hasegawa, J.; Ishida, M.; Nakajima, T.; Honda, Y.; Kitao, O.; Nakai, H.; Klene, M.; Li, X.; Knox, J. E.; Hratchian, H. P.; Cross, J. B.; Adamo, C.; Jaramillo, J.; Gomperts, R.; Stratmann, R. E.; Yazyev, O.; Austin, A. J.; Cammi, R.; Pomelli, C.; Ochterski, J. W.; Ayala, P. Y.; Morokuma, K.; Voth, G. A.; Salvador, P.; Dannenberg, J. J.; Zakrzewski, V. G.; Dapprich, S.; Daniels, A. D.; Strain, M. C.; Farkas, O.; Malick, D. K.; Rabuck,

A. D.; Raghavachari, K.; Foresman, J. B.; Ortiz, J. V.; Cui, Q.; Baboul, A. G.; Clifford, S.; Cioslowski, J.; Stefanov, B. B.; Liu, G.; Liashenko, A.; Piskorz, P.; Komaromi, I.; Martin, R. L.; Fox, D. J.; Keith, T.; Al-Laham, M. A.; Peng, C. Y.; Nanayakkara, A.; Challacombe, M.; Gill, P. M. W.; Johnson, B.; Chen, W.; Wong, M. W.; Gonzalez, C.; Pople, J. A. Gaussian, Inc., Pittsburgh, PA, 2003.

41. Foresman, J. B.; Frisch, E. Exploring Chemistry with Electronic Structure Methods, 2nd ed.; Gaussian: Pittsburgh, 1996.
42. Bosman AW, Janssen HM, Meijer EW. Chem Rev 1999;99:1665–1688. [PubMed: 11849007]
43. Tomalia DA, Naylor AM, Goddard WA III. Angew Chem, Int Ed Engl 1990;29:138–175.
44. Kukowska-Latallo JF, Bielinska AU, Johnson J, Spindler R, Tomalia DA, Baker JR Jr. Proc Natl Acad Sci USA 1996;63:4897–4902. [PubMed: 8643500]
45. Haensler J, Szoka FC. Bioconjugate Chem 1993;4:372–379.
46. He M, McLuckey SA. Rapid Commun Mass Spectrom 2004;18:960–972. [PubMed: 15116423]
47. Wells JM, Chrisman PA, McLuckey SA. J Am Chem Soc 2003;125:7238–7249. [PubMed: 12797797]
48. Su T, Bowers MT. J Am Chem Soc 1973;95:7611–7613.
49. Olmstead WN, Brauman JI. J Am Chem Soc 1977;99:4219–4228.
50. Asubiojo OI, Brauman JI. J Am Chem Soc 1979;101:3715–3724.
51. Reid GE, Wells JM, Badman ER, McLuckey SA. Int J Mass Spectrom 2003;222:243–258.
52. Farrugia JM, O'Hair RAJ. Int J Mass Spectrom 2003;222:229–242.
53. Schnier PD, Price WD, Jockusch RA, Williams ER. J Am Chem Soc 1996;118:7178–7189. [PubMed: 16525512]
54. Ewing NP, Pallante GA, Zhang X, Cassady CJ. J Mass Spectrom 2001;36:875–881. [PubMed: 11523086]
55. Stephenson JL Jr, McLuckey SA. J Am Chem Soc 1997;119:1688–1696.
56. Schnier PD, Gross DS, Williams ER. J Am Chem Soc 1995;117:6747–6757.
57. McLuckey SA, Herron WJ, Stephenson JLJ, Goeringer DE. J Mass Spectrom 1996;31:1093–1100. [PubMed: 8916418]

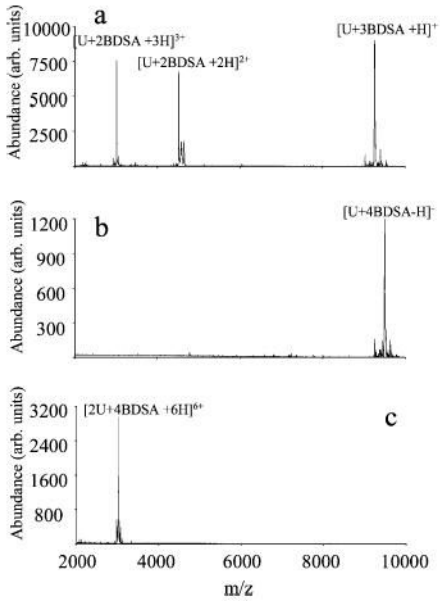

Figure 1.

Ion/ion reaction data for ubiquitin $[U + 7H]^{7+}$ with doubly charged anions derived from BDSA. (a) Spectrum acquired with 300-ms anion accumulation time and 500-ms ion/ion reaction time in positive mode. (b) Spectrum acquired after 700-ms anion accumulation time and 1000-ms ion/ion reaction time in negative mode. (c) Spectrum acquired after ion/ion reaction between singly charged complex anions and $[U + 7H]^{7+}$ ions, which were reintroduced into the trap. The small peaks on either side of the main ion/ion reaction products were also present in the initial isolated ion population.

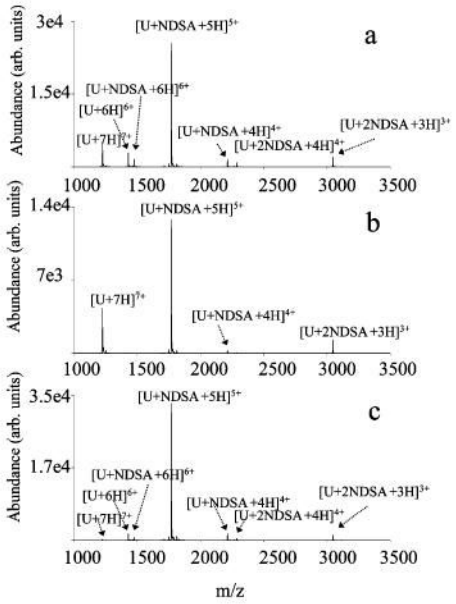

Figure 2.

(a) Positive product ion spectrum after a short ion/ion reaction time for ubiquitin $[U + 7H]^{7+}$ cations and dianions derived from 2,6-NDSA. (b) Positive product ion spectrum obtained under the conditions of (a) while +6 ions were continuously removed from the ion trap via resonance ejection. (c) Positive product ion spectrum obtained under the conditions of (a) while +5 ions were inhibited from undergoing sequential reactions by applying a resonance excitation voltage.

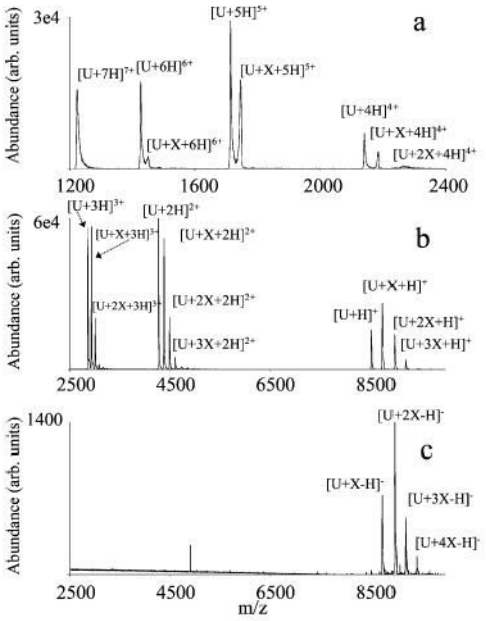

Figure 3.

Ion/ion reaction data for ubiquitin $[U + 7H]^{7+}$ ions and PDPA dianions (a) over the *m*/*z* range between 1200 and 2400 Th in positive mode, (b) over the *m*/*z* range between 2500 and 10000 in positive mode, and (c) over the *m*/*z* range between 2500 and 10000 in negative mode. X represents PDPA.

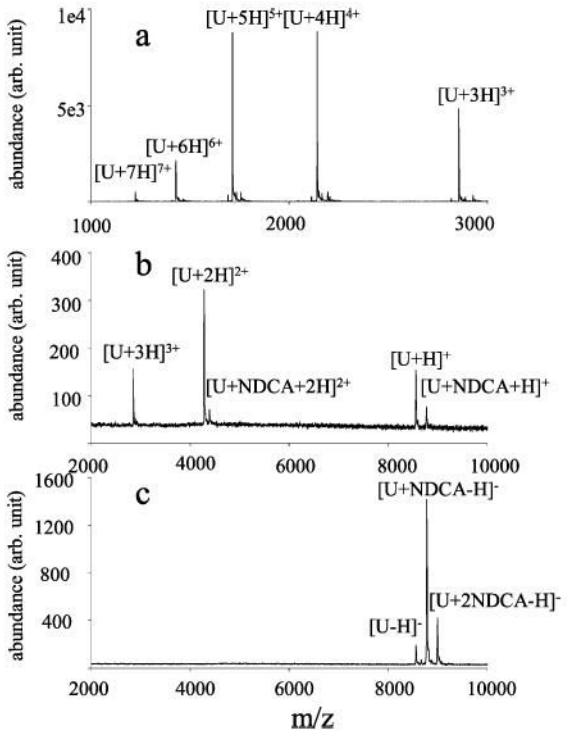

Figure 4.

Product ion data for the reaction of ubiquitin $[U + 7H]^{7+}$ cations with dianions derived from 2,6-NDCA (a) over the *m*/*z* range of 1000–3000 after a relatively short ion/ion reaction period, (b) over the *m*/*z* range of 2000–10 000 acquired after a longer ion/ion reaction period, and (c) over the *m*/*z* range between 2000 and 10 000 in negative mode.

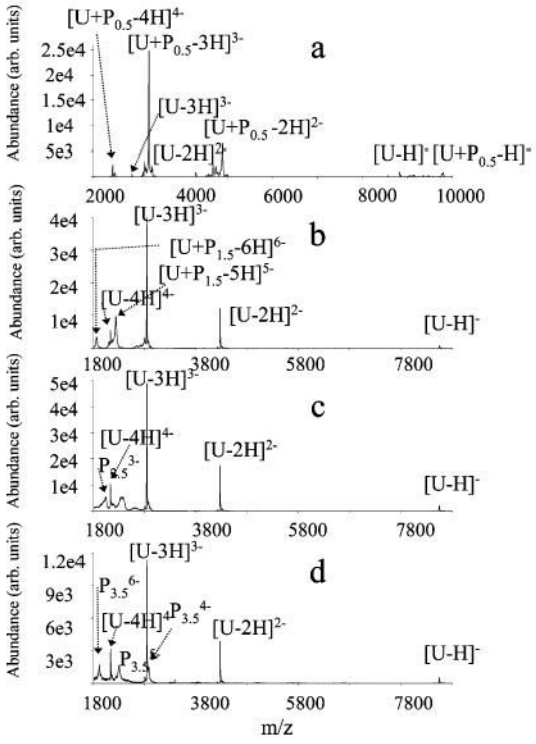

Figure 5.

Negative ion mass spectra collected after ubiquitin $[U + H]^+$ ions subjected to reaction with anions derived from carboxylate-terminated polyamidoamine dendrimer generations 0.5 (a), 1.5 (b), 2.5 (c), and 3.5 (d).

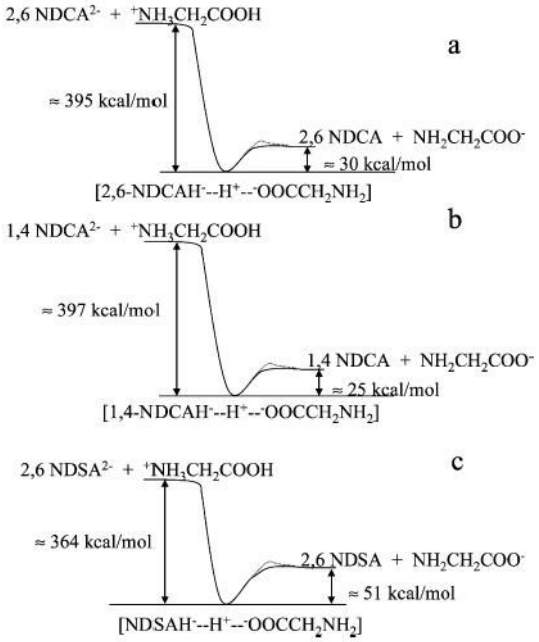

Figure 6.

Calculated energies associated with reactions between singly charged glycine, $NH_3CH_2COOH^+$, with (a) $[2,6\text{-NDCA} - 2H]^{2-}$, (b) $[1,4\text{-NDCA} - 2H]^{2-}$, and (c) $[2,6\text{-NDSA} - 2H]^{2-}$.

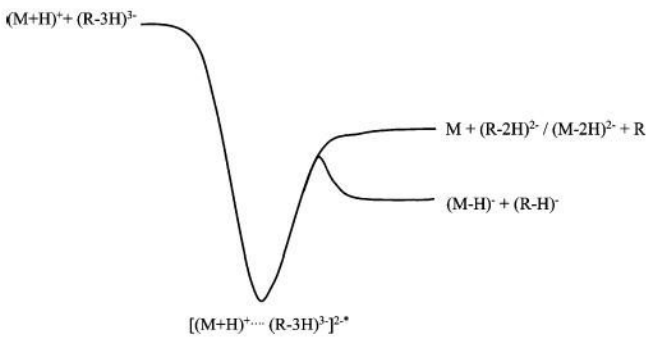

Figure 7.
Hypothetical energy diagram for the case of the reaction of $(M + H)^+$ with $(R - 3H)^{3-}$.

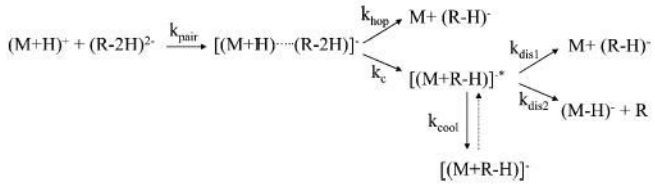

Scheme 1.

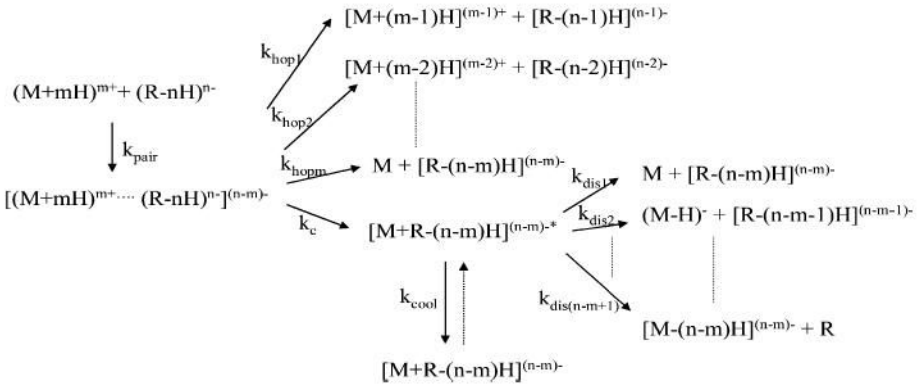

Scheme 2.